Properties of the thalamic projection from the posterior medial nucleus to primary and secondary somatosensory cortices in the mouse

Angela N. Viaene[1], Iraklis Petrof, and S. Murray Sherman

Department of Neurobiology, University of Chicago, Chicago, IL 60637

Edited by Jon H. Kaas, Vanderbilt University, Nashville, TN, and approved October 3, 2011 (received for review September 9, 2011)

Primary somatosensory cortex (S1) receives two distinct classes of thalamocortical input via the lemniscal and paralemniscal pathways, the former via ventral posterior medial nucleus (VPM), and the latter, from the posterior medial nucleus (POm). These projections have been described as parallel thalamocortical pathways. Although the VPM thalamocortical projection has been studied in depth, several details of the POm projection to S1 are unknown. We studied the synaptic properties and anatomical features in the mouse of the projection from POm to all layers of S1 and to layer 4 of secondary somatosensory cortex (S2). Neurons in S1 responded to stimulation of POm with what has been termed Class 2 properties (paired-pulse facilitation, small initial excitatory postsynaptic potentials (EPSPs), a graded activation profile, and a metabotropic receptor component; thought to be modulatory), whereas neurons in layer 4 of S2 responded with Class 1A properties (paired-pulse depression, large initial EPSPs, an all-or-none activation profile, and no metabotropic receptor component, thought to be a main information input). Also, labeling from POm produced small boutons in S1, whereas both small and large boutons were found in S2. Our data suggest that the lemniscal and paralemniscal projections should not be thought of as parallel information pathways to S1 and that the paralemniscal projection may instead provide modulatory inputs to S1.

driver | modulator | glutamatergic | barrel cortex | synapse

Primary somatosensory (also barrel or S1) cortex in rodents receives two distinct types of input from thalamus that are thought to convey different types of sensory information (1, 2). The lemniscal projection is relayed through the ventral posterior medial nucleus (VPM), whereas the paralemniscal projection is routed through posterior medial nucleus (POm) (3, 4). These projections are not only separated in thalamus, but remain largely segregated across cortical layers and in barrels and septa (3–8).

The synaptic properties of the VPM or lemniscal projection to S1 have been described (9–12). VPM inputs to layer 4 and the subgranular layers have Class 1* (or driver) properties, suggesting that they are main information routes, whereas the projections to layers 2/3 have predominantly Class 2 properties, suggesting a modulatory rather than information-bearing function. If the paralemniscal projection to S1 is a parallel information route (3, 4), the prediction is that the synaptic properties of this pathway should be largely or exclusively Class 1A (for detailed explanation of classification terms, see refs. 11–13). POm is known to provide Class 1A input to layer 4 of secondary somatosensory cortex (S2) (10), but the POm projection to S1 has yet to be described. We thus studied the properties of the POm thalamocortical projection and found that the POm projection to S1 is entirely Class 2 in nature, suggesting that it provides modulatory inputs to S1 rather than functioning as a parallel information pathway.

Results

Glutamate Uncaging. We assessed slice connectivity using laser uncaging of glutamate to stimulate POm and recorded the postsynaptic responses from patched cells in cortex (Fig. S1). Inward currents were thus recorded from cells in all layers of S1 and layer 4 of S2 within 6–10 ms following photostimulation. To minimize the potential of electrically activating inappropriate axons, bipolar stimulating electrodes were placed at the site of photostimulation that evoked the largest response in the recorded cortical neuron. All subsequent experiments were performed using electrical stimulation.

Thalamocortical Response Classes. We recorded from a total of 81 neurons in S1 (25 in layers 2/3, 20 in layer 4, 9 in layer 5a, 11 in layer 5b, and 16 in layer 6). Of these neurons, 40 (8 cells in each layer: 2/3, 4, 5a, 5b, and 6) exhibited monosynaptic excitatory postsynaptic potentials (EPSPs) in response to electrical stimulation of POm. The proportion of neurons receiving monosynaptic input from POm was approximately equal in barrel- and septa-associated columns in each subgranular layer of S1 (the numbers in each layer for barrel- and septa-related columns, respectively, are: for layer 5a, 5 of 6 versus 3 of 3; for layer 5b, 5 of 7 versus 3 of 4; and for layer 6, 5 of 10 versus 3 of 6). However, in layers 2/3 and 4, the proportion of cells in barrel-associated columns receiving monosynaptic input from POm (1 of 11 in layers 2/3 and 1 of 9 in layer 4) was much smaller (Mann–Whitney: $P < 0.05$) than neurons in septa-associated columns (7 of 14 in layers 2/3 and 7 of 11 in layer 4). In S2, 10 of 35 recorded cells in layer 4 responded to electrical stimulation of POm with monosynaptic EPSPs. Only the subset of monosynaptically connected cells will be referred to henceforth.

The recorded neurons had membrane potentials of −62.7 ± 5.36 (SD) mV, uncorrected for an approximately −10 mV junction potential, and we found no differences in this parameter either between areas, layers, or barrel/septal regions (Kruskal–Wallis: $P = 0.86$). Differences in input resistance were observed between layers of S1, likely due to the differences in neuron size (average input resistances: layers 2/3, 341.1 ± 122.4 MΩ; layer 4, 512.1 ± 170.3 MΩ; layer 5a, 343.0 ± 81.3 MΩ; layer 5b, 261.1 ± 103.1 MΩ; and layer 6, 500.6 ± 179.5 MΩ). There were no significant differences in membrane resistance between cells associated with barrels and septa in S1 (Mann–Whitney: $P = 0.49$). Neurons in layer 4 of S2 had an input resistance of 463.2 ± 163.2 MΩ. Additionally, all recorded cells exhibited regular spiking in

Author contributions: A.N.V., I.P., and S.M.S. designed research; A.N.V. and I.P. performed research; A.N.V. and I.P. analyzed data; and A.N.V., I.P., and S.M.S. wrote the paper.

The authors declare no conflict of interest.

This article is a PNAS Direct Submission.

[1]To whom correspondence should be addressed. E-mail: angelav@uchicago.edu.

This article contains supporting information online at www.pnas.org/lookup/suppl/doi:10.1073/pnas.1114828108/-/DCSupplemental.

*Several subtypes of Class 1 input have been described (Class 1A, Class 1B, and Class 1C; described in ref. 12). Briefly, Class 1A responses are depressing, have an all-or-none activation profile, and lack a metabotropic glutamate receptor component. Class 1B responses are similar to Class 1A but exhibit a graded activation profile. Class 1C responses show initial facilitation followed by depression and a graded activation profile and lack a metabotropic glutamate receptor component.

response to positive current injection, and all 19 recovered biocytin-filled cells in layers 2/3, 5a, 5b, and 6 were pyramidal.

Average response latency in S1 was 8.13 ± 1.63 ms, whereas average response latency in layer 4 of S2 was 6.34 ± 0.91 ms. The response latencies were significantly larger in recorded cells of S1 than S2 (Mann–Whitney: $P < 0.001$), whereas no significant differences in response latency were observed between layers of S1 (Kruskal–Wallis: $P = 0.35$) or between cells associated with barrels and septa in S1 (Mann–Whitney: $P = 0.27$). Our results are consistent with other studies that observed longer response latencies associated with POm inputs to S1 (14, 15).

All responsive cells in S1 exhibited a Class 2 response pattern (11, 13) to POm stimulation (Fig. 1*A*). That is, these neurons exhibited facilitation in response to trains of stimuli in POm, and as stimulation intensity was increased, the amplitude of the responses also increased (called a graded activation profile, Fig. 1*A*, *i*). EPSPs evoked with 10-Hz stimulation could be blocked by ionotropic glutamate receptor antagonists (Fig. 1*A*, *ii*), and in the presence of those antagonists, high-frequency stimulation (HFS) of POm resulted in a slow, prolonged depolarization that could be blocked with group I metabotropic glutamate receptor antagonists (Fig. 1*A*, *iii*).

This Class 2 response pattern found in cells of S1 sharply contrasts with the responses to POm stimulation recorded in layer 4 of S2, as all cells in layer 4 of S2 responded to POm stimulation with a Class 1A response pattern (Fig. 1*B*). These cells in S2 exhibited depression in response to POm stimulation (Fig. 1*B*, *i*). Increases in stimulation intensity did not cause further increases in EPSP or excitatory postsynaptic current (EPSC) amplitude after a threshold was reached (Fig. 1*B*, *i*). EPSPs evoked at 10 Hz could be blocked by ionotropic glutamate receptor antagonists (Fig. 1*B*, *ii*), and in the presence of these antagonists, high-frequency stimulation of POm failed to activate metabotropic glutamate receptors on these cells (Fig. 1*B*, *iii*). These results are consistent with previous work (10).

Recordings in VPM. To control for the possibility of current spread into VPM activating inputs to layers 2/3 neurons (which could result in Class 2 responses) (11), we performed recordings in 10 VPM neurons while stimulating in POm at various intensities. We found no cells were driven to spike at stimulation intensities used in our experiments or even at higher stimulation intensities (≥400 μA). Most cells showed no response to POm stimulation at any intensity ($n = 8$). Two cells exhibited small EPSPs (<2 mV) at the highest stimulation intensities tested, which were well above the stimulation intensities used in our recordings from cortical neurons (Fig. S2). The most likely explanation for these EPSPs was the activation of layer 6 corticothalamic axons that innervated the VPM cells in question.

Population Data. Fig. 2*A* shows that, among responsive neurons, all cells in S1 showed paired-pulse facilitation (E2/E1 ratios >1), whereas all cells in layer 4 of S2 showed paired-pulse depression (E2/E1 ratios <1). There was no correlation between layer and E2/E1 ratio, and there was a similar variability of this ratio in each layer (Fig. 2*B*). Cells in S1 showed a protracted region of monotonic increases in EPSP amplitude as stimulation intensity was increased (Fig. 2*C*; normalized EPSP amplitude was significantly different across stimulation intensities, Kruskal–Wallis: $P < 0.001$). On the other hand, for cells in layer 4 of S2, once stimulation intensity reached a certain threshold (generally between 50 and 100 μA), further increases in stimulation intensity did not result in further increases in response amplitude (Fig. 2*C*; Kruskal–Wallis: $P = 0.66$). Cells in S1 had an average first EPSP amplitude (evoked at minimum stimulation intensity) of 0.62 ± 0.70 mV, whereas cells in S2 had an average first EPSP amplitude of 6.84 ± 3.67 mV, which was significantly larger (Mann–Whitney: $P < 0.01$). Figure 2*D* is a 3-dimensional scatterplot showing the clustering of properties that distinguish Classes 1A and 2. The parameters involved here are the slope of EPSP amplitude verses stimulation intensity (100 μA and above), amplitudes of the first EPSPs evoked in a train, and a measure of the metabotropic glutamate receptor responses following high-frequency stimulation of POm; this latter variable was taken as the maximum voltage shift from baseline in the 0.25–2 s following cessation of the high-frequency stimulation.

Dual Inputs to S1. While recording responses of S1 neurons to POm stimulation, we also sought to see whether the recorded cells received additional thalamic input from VPM. We found that 22 of the 40 neurons that received monosynaptic inputs from POm also received monosynaptic inputs from VPM. Of these 22

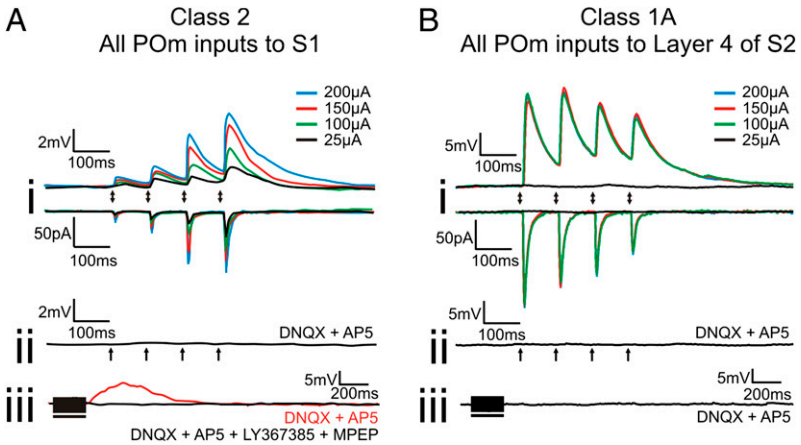

Fig. 1. Examples of Classes 2 and 1A responses. (*A*) Class 2 response pattern. (*A*, *i*) Response to various intensities of thalamic stimulation in current and voltage clamp. (*A*, *ii*) Absence of response following thalamic stimulation at 200 μA in the presence of ionotropic receptor antagonists (DNQX and AP5). (*A*, *iii*) Response to high-frequency stimulation of thalamus at 200 μA in the presence of ionotropic antagonists (red trace) and in the presence of ionotropic and group I metabotropic glutamate receptor antagonists (LY367385 and MPEP, black trace). (*B*) Class 1A response pattern. (*B*, *i*) Response to various intensities of thalamic stimulation in current and voltage clamp. (*B*, *ii*) Absence of response following thalamic stimulation at 200 μA in the presence of ionotropic receptor antagonists. (*B*, *iii*) Absence of response to high-frequency stimulation of thalamus at 200 μA in the presence of ionotropic antagonists. Arrows represent the timing of stimulation for all low-frequency stimulation trials. Black bars represent the duration of stimulation in high-frequency stimulation trials. With the exception of high-frequency stimulation trials, all traces represent the average of 10 sweeps.

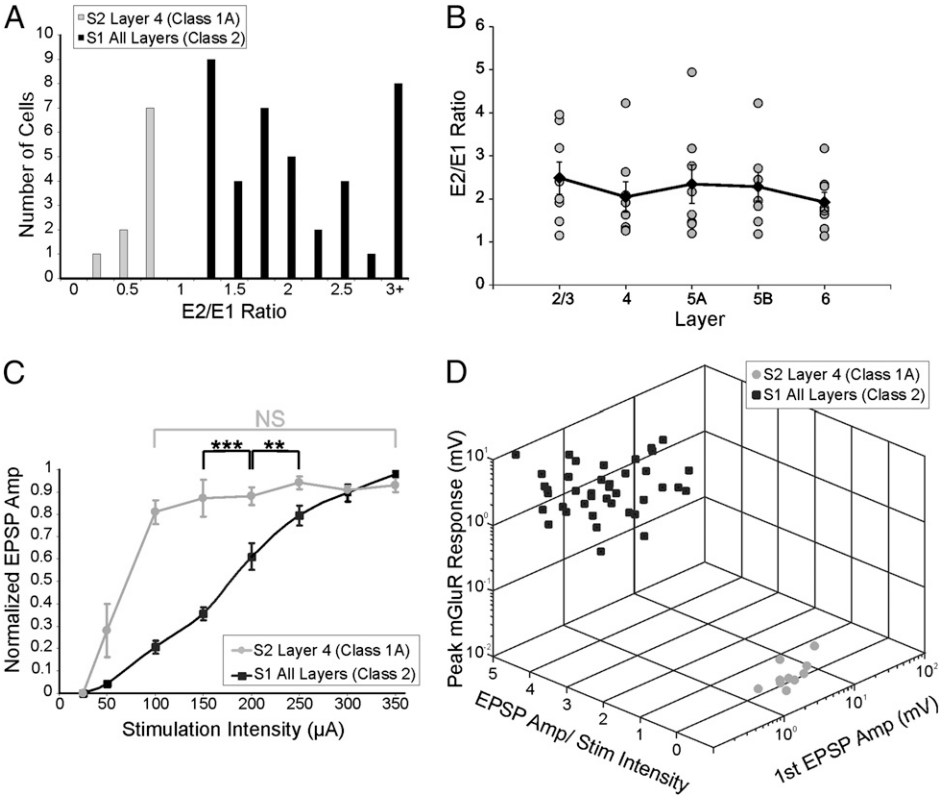

Fig. 2. Summary of response properties. (*A*) Ratio of amplitude of second to first EPSP (E2/E1 ratio) of neurons in S1 and layer 4 of S2. (*B*) E2/E1 ratios of neurons in S1 grouped by layer. Gray circles represent individual E2/E1 ratios. Black diamonds represent the average E2/E1 ratio for each layer. Error bars are SEM. (*C*) Relationship between normalized EPSP amplitude and stimulation intensity. Error bars represent SEM. $^{**}P < 0.01$, $^{***}P < 0.001$; NS, not significant. (*D*) 3D scatterplot of response properties of neurons in S1 and layer 4 of S2.

neurons, 2 were located in layers 2/3, 6 within layer 4, 7 within layer 5A, 4 within layer 5B, and 3 within layer 6. In response to VPM stimulation, all layers 4, 5A, 5B, and 6 neurons responded with Class 1 properties (specifically, these were Class 1A for all cells in layer 4, and either Class 1A, 1B, or 1C for each cell in the subgranular layers) and Class 2 properties following POm stimulation, whereas the layers 2/3 neurons responded with Class 2 properties following both VPM (11) and POm stimulation (Fig. S3).

Bouton Sizes. Biotinylated dextran amine (BDA) injections in POm produced extensive anterograde labeling in both S1 and S2 (Fig. 3*B*). Some retrograde labeling was also observed in cells of layer 5 in both S1 and S2, whereas retrograde labeling in layer 6 was only observed in S2. S1 contained smaller boutons, whereas layer 4 of S2 labeling revealed both large and small boutons. Average bouton size in all layers of S1 ($0.71 \pm 0.29\ \mu m^2$) was significantly smaller than in layer 4 of S2 ($0.98 \pm 0.47\ \mu m^2$) (Fig. 3 *C*–*E*; Mann–Whitney: $P < 0.001$). No differences in bouton size were observed between layers of S1 (Kruskal–Wallis: $P = 0.64$) or in columns associated with barrels and septa in S1 (Mann–Whitney: $P = 0.94$). A correlation between bouton size and pathways associated with Classes 1A and 2 properties has been reported before (11, 13, 16), and we observed a similar correlation in this study where Class 2 inputs and smaller boutons were observed in S1 with Class 1A inputs and larger boutons, in layer 4 of S2.

Additionally, we found that the average bouton size in layers 2/3 of S2 ($0.83 \pm 0.26\ \mu m^2$) was significantly smaller than in layer 4 of S2 (Mann–Whitney: $P < 0.001$). The size of the boutons in layers 2/3 of S2 following POm injection was similar to the measured size of boutons in layers 2/3 of S1 following VPM injection (11). However, despite the smaller boutons in layers 2/3 of S2, the average bouton size in S2 ($1.24 \pm 0.58\ \mu m^2$) was significantly larger than average bouton size in S1 (Fig. 3*E*; Mann–Whitney: $P < 0.001$).

Discussion

We found that stimulation of POm resulted in distinctly different response patterns in S1 and S2. All responses recorded in S1 were Class 2 in nature, whereas the responses in layer 4 of S2 were Class 1A. Class 2 response properties consist of facilitation, smaller initial EPSPs, a graded activation profile, and a metabotropic component, whereas Class 1A responses are defined by depression, larger first EPSPs, all-or-none responses, and the absence of a metabotropic component. Our previous suggestion is that Class 1A responses, previously called drivers, are a main information route, whereas Class 2 responses, previously called modulators, provide mainly modulatory functions (11, 17, 18).

We also found anatomical differences in the POm projection to S1 and S2. Boutons in S1 were smaller, whereas both large and small boutons were found in layer 4 of S2. These anatomical findings are consistent with previous work that found a range of small to large boutons for projections with Class 1A properties and only small boutons for projections with Class 2 properties (11, 13, 19–22). Within S1, we found no differences in response properties or bouton sizes between layers of cortex or between barrel and septal-related columns. Additionally, the presence of smaller boutons in layers 2/3 of S2 and larger boutons in the subgranular layers of S2 is consistent with known properties of the VPM-to-S1 projection (11, 12). Class 1A inputs to layer 4 of S2 as well as the anatomical data suggest that the POm-to-S2 projection may be similar in function to the VPM-to-S1 projection.

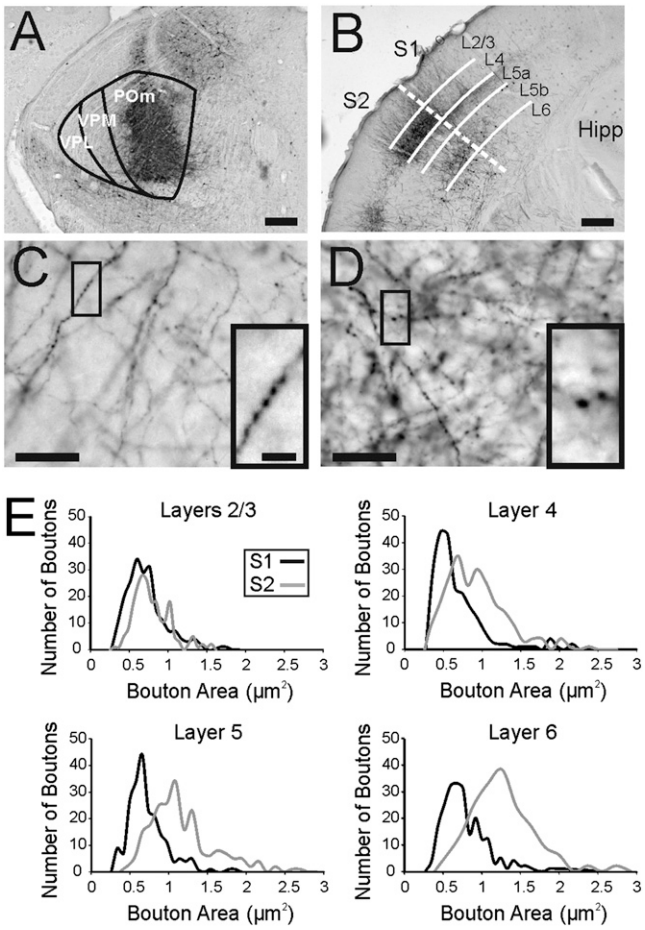

Fig. 3. Anterograde tracing of thalamic BDA injections. (*A*) Example of thalamic injection site in POm. (*B*) Example of anterograde labeling of axons and boutons in S1 and S2. Dashed line marks border of S1 and S2 and solid lines mark borders between layers. (*C*) BDA-labeled axons and boutons in S1. Highlighted area shown at higher magnification in *Inset*. (*D*) BDA-labeled axons and boutons in layer 4 of S2. Highlighted area shown at higher magnification in *Inset*. (*E*) Histograms of bouton area in different layers of S1 and S2. (Scale bars in *A* and *B*, 0.25 mm; in *C* and *D*, 25 μm; in *C* and *D* *Insets*, 5 μm.)

Although POm projections to S1 are concentrated in layers 1 and 5a and in the septa of layers 2/3 and 4 (present study and refs. 3 and 8), we found cells in all layers of S1 that received input from POm. An important proviso is that we recorded the location of cell bodies, and because most of these were pyramidal cells (the most common excitatory cell type in cortex; ref 23) with apical dendrites spanning many layers dorsally, the actual laminar location of the synaptic input cannot be specified. Indeed, on the basis of anatomical studies, all excitatory neurons in layers 2–6 of S1 potentially receive synaptic inputs from POm (7, 24).

Anitdromic Activation and Current Spread. We can rule out the likelihood of antidromic activation as a factor here for a number of reasons. If antidromic activation of layer 5 neurons was the driving force behind the recorded responses, we should have seen antidromic activation in several of our recorded layer 5 neurons. As we have never observed antidromic activation in layer 5 neurons at stimulation intensities used in these experiments, we feel that it is highly unlikely for our responses to be due to antidromic activation. Additionally, previous work has shown that antidromic activation of corticothalamic fibers requires much higher stimulation intensities (>300 μA) than orthodromic activation of thalamocortical projections (25), supporting our conclusions.

It is unlikely that the responses we recorded in layers 2/3 neurons resulted from current spread into VPM. No neurons in VPM were driven to spike following POm stimulation, even at intensities much higher than those used during recordings from S1 neurons (Fig. S2). Additionally, given that current spread that activates VPM inputs would result in Class 1 responses measured in layers 4–6 (which was never observed), we feel it is highly unlikely that any of our recorded responses are due to current spread into VPM.

Origins of POm Projections. As the POm inputs to S1 and layer 4 of S2 have distinct properties, a question remains as to whether or not these projections arise from two distinct populations of thalamic neurons. Another possibility is that the same relay cell in thalamus can provide Class 2 input to S1 and Class 1A input to S2 via a branched axon. The presence of cells in POm that project to both S1 and S2 has been described; however, they are quite sparse (26). Bouton measurements suggest that POm may be providing Class 2 inputs to layers 2/3 of S2. Therefore, POm cells that project to both S1 and S2 could potentially be providing modulatory input to both areas. The origins of Class 1A and Class 2 inputs remain an issue to be resolved.

Inputs to POm Relay Cells. It has been well documented in in vivo studies that stimulation of whiskers activates both the lemniscal and paralemniscal pathways resulting in responses throughout S1 in both barrels and septa (1, 2, 14, 15). In the paralemniscal pathway, POm receives ascending sensory input from the subnuclei of the spinal trigeminal complex (27, 28). POm receives Class 1A input from layer 5 of S1 (29) and also receives input from layers 5 and 6 of S2 (30). It is unknown whether any of these corticothalamic projections target relay cells that project to S1; however, these patterns of connectivity provide a possible means for S2 to provide modulatory feedback projections to S1 via the thalamus or for S1 itself to activate these modulatory inputs.

Comparison with Other Species and Sensory Systems. Pathways that resemble the paralemniscal projection in the rodent somatosensory system have been described in several other species and in different sensory systems. The anterior pulvinar of monkeys is thought to be analogous (and perhaps homologous) to POm of rodents, and it projects not only to S2, but to S1 as well (31). Our findings regarding the POm projections to S1 and S2 may offer insights to the nature of these anterior pulvinar projections in primates.

Additionally, it has been proposed that there may be a pathway analogous to the somatosensory paralemniscal projection in the primate auditory system (32), with a projection through different divisions of the medial geniculate body to primary auditory cortex, and this auditory paralemniscal pathway has also been described in cats and guinea pigs (33, 34). The projection is thought of as a parallel information pathway to the auditory lemniscal pathway (much like in the somatosensory system); however, our results suggest that, whereas these pathways appear to be parallel anatomically, they may not be functionally equivalent.

In the visual system of primates, the pulvinar is a higher-order thalamic nucleus (analogous to POm in the rodent somatosensory system). The pulvinar is known to send projections to both primary (V1) and secondary visual cortices (35, 36). These projections led Rezak and Benevento (36) to conclude that the inputs from pulvinar are likely to influence the response properties of V1 neurons. Despite this insight, the projection from pulvinar to V1 is poorly understood. Although the projection from the lateral geniculate nucleus provides driving input to V1 (17, 37), our findings suggest the possibility that the projection

from pulvinar may be acting to modulate these ascending driving inputs.

Information Flow via Transthalamic Pathways. Attention has been focused recently on the role of higher order thalamic nuclei, such as POm, as an integral link in a transthalamic route for corticocortical communication (10). Implicit in this concept is the idea that these transthalamic circuits are feed forward, such as from S1 to S2, and there is indeed evidence for this (38). However, the possibility exists that transthalamic circuits can also be organized as feedback pathways. If the hypothesis is correct that Class 1 inputs underlie basic information flow, and Class 2 inputs are modulatory in function (17, 18), then our present data suggest that POm is not a link in a feedback transthalamic information route to S1.

Role of POm Inputs to S1 and S2. In thalamus, drivers (Class 1A inputs) provide receptive field-defining inputs to their postsynaptic targets, whereas modulators (Class 2 inputs) affect how driving input is relayed (reviewed in refs. 17 and 18). Our findings are consistent with previous work that described POm inputs to layer 4 of S2 as driver-like (10). As neurons in S1 responded to POm stimulation with only Class 2 response properties, we suggest that the role of the paralemniscal projection is to provide modulatory inputs to barrel cortex. This leads us to conclude that the paralemniscal projection is not a parallel information pathway to S1; rather it functions to modulate the driving inputs provided to S1 by the lemniscal pathway.

Materials and Methods

We adopted our previously described techniques (10, 11), which are briefly described here.

Slice Preparation. Thalamocortical slices were prepared from BALB/c mice (aged 9–18 d). Animals were deeply anesthetized with isolfluorane and were then decapitated. Brains were removed and placed in cold (0–4 °C), oxygenated (95% O_2–5% CO_2) slicing solution containing (in millimoles): 2.5 KCl, 1.25 NaH_2PO_4, 10 $MgCl_2$, 0.5 $CaCl_2$, 26 $NaHCO_3$, 11 glucose, and 206 sucrose. Thalamocortical slices (500 μm thick) were prepared as described before (9) and were kept in artificial cerebrospinal fluid containing (in millimoles) 125 NaCl, 3 KCl, 1.25 NaH_2PO_4, 1 $MgCl_2$, 2 $CaCl_2$, 25 $NaHCO_3$, and 25 glucose at room temperature. All procedures were carried out in accordance with guidelines by the institutional animal care and use committee of the University of Chicago.

Electrophysiology. Whole-cell recordings were performed in a visualized slice setup under a differential interference contrast (DIC)-equipped microscope to visualize thalamic and cortical structures. Current- and voltage-clamp signals were collected and amplified using pCLAMP software and a Multiclamp 700B amplifier (Axon Instruments).

Recording glass pipettes (input resistances 3–7 MΩ) were filled with intracellular solution containing (in millimoles) 117 K-gluconate, 13 KCl, 1 $MgCl_2$, 0.07 $CaCl_2$, 10 Hepes, 0.1 EGTA, 2 Na_2-ATP, 0.4 Na-GTP, 0.02% biocytin, and 0.003 of the chloride channel blocker TS-TM calix[4]arene (generously provided by R. J. Bridges, Rosalind Franklin University, Chicago); pH 7.3, 290 mOsm. Slices were processed for biocytin as previously described (11).

Individual cortical layers and areas corresponding to barrels and septa were identified under DIC. Transition zones between layers or between barrels and septa were avoided to minimize the risk of false sampling. Electrical stimulation of POm was delivered by a concentric bipolar electrode (FHC).

The assessment of short-term plasticity (depression versus facilitation) was carried out by using a stimulation protocol consisting of four, 0.1-ms-long positive current pulses at a frequency of 10 Hz. Initially this was done only for the lowest stimulation intensity capable of inducing excitatory postsynaptic potentials (EPSPs) of a >0.5 mV amplitude (for ≥3 of the four EPSPs) in the recorded cells. Subsequently, however, we also examined the effects of increased stimulation currents on evoked responses (*Results*).

To induce and isolate metabotropic glutamate receptor activation, we used a high-frequency stimulation protocol (0.1-ms-long pulses delivered at 125 Hz over 200–800 ms, 100–300 μA) (39) combined with the application of NMDA and AMPA receptor antagonists (100 μM of AP5 and 50 μM of DNQX, respectively). Where necessary, we used the type 1 metabotropic glutamate receptor antagonist LY367385 (40 μM) and the type 5 metabotropic glutamate receptor antagonist MPEP (30 μM) (collectively known as group I metabotropic glutamate receptor antagonists). All data were digitized on a Digidata 1200 board (Axon Instruments) and analyzed in ClampFit (Axon Instruments) software.

The latency of an EPSP was measured as the time between stimulation offset and the initiation of the evoked EPSP. We used criteria described before (11, 12) to assess the monosynaptic nature of the recorded responses. E2/E1 ratio was calculated by dividing the amplitude of the second EPSP by the amplitude of the first EPSP. An E2/E1 ratio >1 indicates paired-pulse facilitation, whereas an E2/E1 ratio <1 indicates paired-pulse depression.

Glutamate Photo-Uncaging. Nitroindolinyl-caged glutamate (Sigma-Aldrich) was added to the recirculating artificial cerebrospinal fluid (0.4 mM) for the experiments requiring glutamate photo-uncaging. A UV laser beam (DPSS Laser) was used to locally photolyse the caged compound over an 8 × 8 grid in a pseudorandom order (40–43). The laser beam had an intensity of 20–80 mW, and the laser illumination lasted 2 ms (355 nm wavelength, frequency-tripled Nd:YVO4, 100-kHz pulse repetition rate). Custom-made software written in Matlab (Mathworks) was used to control the uncaging interface.

Surgery and Neuroanatomical Techniques. The animals were anesthetized with a mixture of ketamine (100 mg/kg) and xylazine (3 mg/kg) and placed in a surgical stereotaxic frame (Kopf). Stereotaxic coordinates for the injection of anterograde tracers into POm were determined using the Franklin and Paxinos (44) mouse brain atlas (all distances are from Bregma): anteroposterior, −2.06; mediolateral, ±1.25; and dorsoventral, −3.15. Bilateral injections of 5% BDA 10,000 MW, Molecular Probes) in PBS were performed through iontophoresis (5–12 μA, 7-s-long on–off cycles, for 15–20 min).

After a 72-h recovery period, the animals were deeply anesthetized with ketamine/xylazine and transcardially perfused with PBS followed by 4% paraformaldyhyde in PBS. Brains were saturated in 10–30% sucrose in PFA overnight and 35-μm-thick coronal sections were cut using a sliding microtome. Slices were processed for BDA as described in Viaene et al. (11). After processing, sections were mounted onto gelatinized slides, dehydrated, and coverslipped.

Brain sections were examined under a microscope (Leica Microsystems), and photos of terminal fields in all layers of S1 and layer 4 of S2 were taken at 100× using a Retiga2000 monochrome CCD camera and QCapture Pro software (QImaging). The resolution of the digital images used for the bouton area measurements was 1,600 × 1,200 pixels, and the size of each pixel was 0.075 μm. The plane of focus was determined by the researcher taking the photos.

After a photo was taken and code named to avoid bias, identified patterns of axons and/or boutons at the edges of the photo were used as landmarks for transitioning to directly adjacent areas within the region of interest before the next photo was taken, ensuring that boutons did not appear in multiple photos. AxioVision software (Carl Zeiss Instruments) was used to analyze the coded images and measure the sizes of boutons. Labeled boutons were identified by their round shape and were marked by manually outlining their perimeter, which also prevented repetitive counting. The limits of the resolution at the light microscopic level with our combination of magnification and numerical aperture have been estimated to be around 0.3 μm (22, 45, 46). We excluded any bouton with a diameter of <0.4 μm from our measurements. We focused our measurements on layers 2/3, 4, 5a, 5b, and 6 of S1 and layer 4 of S2. We counted 200 boutons per layer in S1 (100 in a barrel or a barrel-related column and 100 in the septa or areas aligned with a septa), 1,000 boutons in layer 4 of S2, 500 in layers 2/3 of S2, and 200 each in layers 5a, 5b, and 6 of S2. For comparing bouton sizes between S1 and S2, 1,000 boutons each from S1 and S2 were used in the calculations (200 boutons from each layer of each area).

ACKNOWLEDGMENTS. This work was supported by National Institute on Deafness and Other Communication Disorders Grant DC008794 (to S.M.S.) and National Institute of General Medical Sciences Medical Scientist National Research Service Award 5 T32 GM07281 (to A.N.V.).

1. Ahissar E, Sosnik R, Haidarliu S (2000) Transformation from temporal to rate coding in a somatosensory thalamocortical pathway. *Nature* 406:302–306.
2. Yu C, Derdikman D, Haidarliu S, Ahissar E (2006) Parallel thalamic pathways for whisking and touch signals in the rat. *PLoS Biol* 4:e124.
3. Lu SM, Lin RC (1993) Thalamic afferents of the rat barrel cortex: A light- and electron-microscopic study using Phaseolus vulgaris leucoagglutinin as an anterograde tracer. *Somatosens Mot Res* 10:1–16.
4. Koralek KA, Jensen KF, Killackey HP (1988) Evidence for two complementary patterns of thalamic input to the rat somatosensory cortex. *Brain Res* 463:346–351.
5. Woolsey TA, Van der Loos H (1970) The structural organization of layer IV in the somatosensory region (SI) of mouse cerebral cortex. The description of a cortical field composed of discrete cytoarchitectonic units. *Brain Res* 17:205–242.
6. Bureau I, von Saint Paul F, Svoboda K (2006) Interdigitated paralemniscal and lemniscal pathways in the mouse barrel cortex. *PLoS Biol* 4:e382.
7. Meyer HS, et al. (2010) Cell type-specific thalamic innervation in a column of rat vibrissal cortex. *Cereb Cortex* 20:2287–2303.
8. Wimmer VC, Bruno RM, de Kock CP, Kuner T, Sakmann B (2010) Dimensions of a projection column and architecture of VPM and POm axons in rat vibrissal cortex. *Cereb Cortex* 20:2265–2276.
9. Agmon A, Connors BW (1991) Thalamocortical responses of mouse somatosensory (barrel) cortex in vitro. *Neuroscience* 41:365–379.
10. Lee CC, Sherman SM (2008) Synaptic properties of thalamic and intracortical inputs to layer 4 of the first- and higher-order cortical areas in the auditory and somatosensory systems. *J Neurophysiol* 100:317–326.
11. Viaene AN, Petrof I, Sherman SM (2011) Synaptic properties of thalamic input to layers 2/3 and 4 of primary somatosensory and auditory cortices. *J Neurophysiol* 105: 279–292.
12. Viaene AN, Petrof I, Sherman SM (2011) Synaptic properties of thalamic input to the subgranular layers of primary somatosensory and auditory cortices in the mouse. *J Neurosci* 31:12738–12747.
13. Covic EN, Sherman SM (2011) Synaptic properties of connections between the primary and secondary auditory cortices in mice. *Cereb Cortex* 21:2425–2441.
14. Brecht M, Roth A, Sakmann B (2003) Dynamic receptive fields of reconstructed pyramidal cells in layers 3 and 2 of rat somatosensory barrel cortex. *J Physiol* 553: 243–265.
15. Brecht M, Sakmann B (2002) Dynamic representation of whisker deflection by synaptic potentials in spiny stellate and pyramidal cells in the barrels and septa of layer 4 rat somatosensory cortex. *J Physiol* 543:49–70.
16. Li J, Guido W, Bickford ME (2003) Two distinct types of corticothalamic EPSPs and their contribution to short-term synaptic plasticity. *J Neurophysiol* 90:3429–3440.
17. Sherman SM, Guillery RW (1998) On the actions that one nerve cell can have on another: Distinguishing "drivers" from "modulators." *Proc Natl Acad Sci USA* 95: 7121–7126.
18. Sherman SM, Guillery RW (2006) *Exploring the Thalamus* (MIT Press, Cambridge).
19. Keller A, White EL, Cipolloni PB (1985) The identification of thalamocortical axon terminals in barrels of mouse Sml cortex using immunohistochemistry of anterogradely transported lectin (Phaseolus vulgaris-leucoagglutinin). *Brain Res* 343: 159–165.
20. Sur M, Esguerra M, Garraghty PE, Kritzer MF, Sherman SM (1987) Morphology of physiologically identified retinogeniculate X- and Y-axons in the cat. *J Neurophysiol* 58:1–32.
21. Van Horn SC, Sherman SM (2004) Differences in projection patterns between large and small corticothalamic terminals. *J Comp Neurol* 475:406–415.
22. Llano DA, Sherman SM (2008) Evidence for nonreciprocal organization of the mouse auditory thalamocortical-corticothalamic projection systems. *J Comp Neurol* 507: 1209–1227.
23. Lorente de Nó R (1949) Cerebral cortex: Architecture, intracortical connections and motor projections. *Physiology of the Nervous System*, ed Fulton JF (Oxford Univ Press, Oxford), 3rd Ed, pp 288–330.
24. White EL (1978) Identified neurons in mouse Sml cortex which are postsynaptic to thalamocortical axon terminals: A combined Golgi-electron microscopic and degeneration study. *J Comp Neurol* 181:627–661.
25. Beierlein M, Connors BW (2002) Short-term dynamics of thalamocortical and intracortical synapses onto layer 6 neurons in neocortex. *J Neurophysiol* 88:1924–1932.
26. Spreafico R, Barbaresi P, Weinberg RJ, Rustioni A (1987) SII-projecting neurons in the rat thalamus: A single- and double-retrograde-tracing study. *Somatosens Res* 4: 359–375.
27. Veinante P, Deschênes M (1999) Single- and multi-whisker channels in the ascending projections from the principal trigeminal nucleus in the rat. *J Neurosci* 19:5085–5095.
28. Pierret T, Lavallée P, Deschênes M (2000) Parallel streams for the relay of vibrissal information through thalamic barreloids. *J Neurosci* 20:7455–7462.
29. Reichova I, Sherman SM (2004) Somatosensory corticothalamic projections: Distinguishing drivers from modulators. *J Neurophysiol* 92:2185–2197.
30. Lévesque M, Gagnon S, Parent A, Deschênes M (1996) Axonal arborizations of corticostriatal and corticothalamic fibers arising from the second somatosensory area in the rat. *Cereb Cortex* 6:759–770.
31. Krubitzer LA, Kaas JH (1992) The somatosensory thalamus of monkeys: Cortical connections and a redefinition of nuclei in marmosets. *J Comp Neurol* 319:123–140.
32. Rauschecker JP, Tian B, Pons T, Mishkin M (1997) Serial and parallel processing in rhesus monkey auditory cortex. *J Comp Neurol* 382:89–103.
33. He J, Hashikawa T, Ojima H, Kinouchi Y (1997) Temporal integration and duration tuning in the dorsal zone of cat auditory cortex. *J Neurosci* 17:2615–2625.
34. Abrams DA, Nicol T, Zecker S, Kraus N (2011) A possible role for a paralemniscal auditory pathway in the coding of slow temporal information. *Hear Res* 272:125–134.
35. Ogren MP, Hendrickson AE (1977) The distribution of pulvinar terminals in visual areas 17 and 18 of the monkey. *Brain Res* 137:343–350.
36. Rezak M, Benevento LA (1979) A comparison of the organization of the projections of the dorsal lateral geniculate nucleus, the inferior pulvinar and adjacent lateral pulvinar to primary visual cortex (area 17) in the macaque monkey. *Brain Res* 167:19–40.
37. Guillery RW, Sherman SM (2002) Thalamic relay functions and their role in corticocortical communication: Generalizations from the visual system. *Neuron* 33:163–175.
38. Theyel BB, Llano DA, Sherman SM (2010) The corticothalamocortical circuit drives higher-order cortex in the mouse. *Nat Neurosci* 13:84–88.
39. McCormick DA, von Krosigk M (1992) Corticothalamic activation modulates thalamic firing through glutamate "metabotropic" receptors. *Proc Natl Acad Sci USA* 89: 2774–2778.
40. Lam YW, Sherman SM (2005) Mapping by laser photostimulation of connections between the thalamic reticular and ventral posterior lateral nuclei in the rat. *J Neurophysiol* 94:2472–2483.
41. Lam YW, Nelson CS, Sherman SM (2006) Mapping of the functional interconnections between thalamic reticular neurons using photostimulation. *J Neurophysiol* 96: 2593–2600.
42. Lam YW, Sherman SM (2007) Different topography of the reticulothalmic inputs to first- and higher-order somatosensory thalamic relays revealed using photostimulation. *J Neurophysiol* 98:2903–2909.
43. Shepherd GM, Pologruto TA, Svoboda K (2003) Circuit analysis of experience-dependent plasticity in the developing rat barrel cortex. *Neuron* 38:277–289.
44. Franklin KBJ, Paxinos G (2008) *The Mouse Brain in Stereotaxic Coordinates* (Academic, San Diego).
45. Slayter E (1970) *Optical Methods in Biology* (Wiley-Interscience, New York).
46. Friedlander MJ, Lin CS, Stanford LR, Sherman SM (1981) Morphology of functionally identified neurons in lateral geniculate nucleus of the cat. *J Neurophysiol* 46:80–129.